Environmental Research Letters

LETTER

Response of ecosystem intrinsic water use efficiency and gross primary productivity to rising vapor pressure deficit

Quan Zhang[1,2,9], **Darren L Ficklin**[3], **Stefano Manzoni**[4,5], **Lixin Wang**[6], **Danielle Way**[7], **Richard P Phillips**[8] **and Kimberly A Novick**[2]

[1] State Key Laboratory of Water Resources and Hydropower Engineering Science, Wuhan University, Wuhan, People's Republic of China
[2] School of Public and Environmental Affairs, Indiana University, Bloomington, IN, United States of America
[3] Department of Geography, Indiana University, Bloomington, IN, United States of America
[4] Department of Physical Geography, Stockholm University, Stockholm, Sweden
[5] Bolin Center for Climate Research, Stockholm University, Stockholm, Sweden
[6] Department of Earth Sciences, Indiana University-Purdue University Indianapolis (IUPUI), Indianapolis, IN, United States of America
[7] Department of Biology, University of Western Ontario, London, Ontario, Canada
[8] Department of Biology, Indiana University, Bloomington, IN, United States of America
[9] Author to whom any correspondence should be addressed.

E-mail: quan.zhang@whu.edu.cn **and** quazhang@indiana.edu

OPEN ACCESS

RECEIVED
4 January 2019

REVISED
1 April 2019

ACCEPTED FOR PUBLICATION
31 May 2019

PUBLISHED
12 July 2019

Keywords: hydrologic stress, FLUXNET, stomatal closure, water use

Supplementary material for this article is available online

Abstract

Elevated vapor pressure deficit (VPD) due to drought and warming is well-known to limit canopy stomatal and surface conductance, but the impacts of elevated VPD on ecosystem gross primary productivity (GPP) are less clear. The intrinsic water use efficiency (iWUE), defined as the ratio of carbon (C) assimilation to stomatal conductance, links vegetation C gain and water loss and is a key determinant of how GPP will respond to climate change. While it is well-established that rising atmospheric CO_2 increases ecosystem iWUE, historic and future increases in VPD caused by climate change and drought are often neglected when considering trends in ecosystem iWUE. Here, we synthesize long-term observations of C and water fluxes from 28 North American FLUXNET sites, spanning eight vegetation types, to demonstrate that ecosystem iWUE increases consistently with rising VPD regardless of changes in soil moisture. Another way to interpret this result is that GPP decreases less than surface conductance with increasing VPD. We also project how rising VPD will impact iWUE into the future. Results vary substantially from one site to the next; in a majority of sites, future increases in VPD (RCP 8.5, highest emission scenario) are projected to increase iWUE by 5%–15% by 2050, and by 10%–35% by the end of the century. The increases in VPD owing to elevated global temperatures could be responsible for a 0.13% $year^{-1}$ increase in ecosystem iWUE in the future. Our results highlight the importance of considering VPD impacts on iWUE independently of CO_2 impacts.

Introduction

Given that plants are constantly challenged to maximize carbon (C) uptake and minimize water loss by regulating stomata, an important metric of ecosystem sensitivity to climate is the intrinsic water use efficiency (iWUE), defined here as the ratio of C assimilation (A_n) to stomatal conductance (g_s). The iWUE reflects plants' adaptability to changing environmental conditions (Farquhar *et al* 1982), and because it ultimately governs the coupling between carbon assimilation and stomatal conductance, it has received considerable attention (Keenan *et al* 2013, Lévesque *et al* 2014, Frank *et al* 2015, van der Sleen *et al* 2015). Recently, increasing iWUE has been observed in many ecosystems. This phenomenon has largely been attributed to rising atmospheric CO_2 concentrations (Franks *et al* 2013), a conclusion supported by both observational studies (Ainsworth and Long 2005, Battipaglia *et al* 2013, Keenan *et al* 2013,

Mastrotheodoros *et al* 2017) and theoretical models (Knauer *et al* 2017b). However, homeostatic iWUE has also been reported (Marshall and Monserud 1996, Wu *et al* 2015, Wieser *et al* 2016), and models and experiments frequently show diverse patterns of iWUE response to rising CO_2 (Keenan *et al* 2013, Knauer *et al* 2017b). While many factors could explain this disagreement, among them is the possibility that CO_2 may not be the only slowly-evolving driver affecting iWUE.

The balance between vegetative carbon uptake and water loss is also affected by moisture deficits in the soil and the atmosphere. Theory predicts, and some data confirm, that iWUE should increase when water availability is low (Gomes *et al* 2009, Schultz and Stoll 2010, de Santana *et al* 2015). The extent to which changes in atmospheric evaporative demand (i.e. vapor pressure deficit; VPD) can affect iWUE independently of changes in soil moisture (Schultz and Stoll 2010, Lévesque *et al* 2014, Tomas *et al* 2014, Kwon *et al* 2017) is less understood. Unlike the total water use efficiency (WUE = assimilation/transpiration), the iWUE describes plant responses to rising VPD without being confounded by the abiotic increase in evaporative potential when VPD is high. Consequently, even though total WUE could decline during drought, iWUE would increase. Quantifying the sensitivity of iWUE to VPD is particularly important for understanding the response of gross primary productivity (GPP) to VPD, as VPD has been rising in many places, and is expected to increase further in most biomes as temperatures continue to rise (Ficklin and Novick 2017).

Plant physiological theory offers some important clues as to how iWUE should respond to rising VPD. Because the intercellular CO_2 concentration (c_i) is strongly controlled by stomatal conductance (Farquhar and Wong 1984), and because the relationship between A_n and c_i is hyperbolic, the relationship between A_n and g_s is also hyperbolic. As VPD initially begins to rise, g_s will be reduced, but the rate of and biochemical potential for photosynthesis may be unaffected because of the sufficiently atmospheric CO_2 supply. In this case, iWUE is expected to increase. However, if VPD-driven reductions in g_s (and thus c_i) become more severe, reducing photosynthetic rates, or if coincident reductions in soil moisture limit biochemical capacity, then iWUE may stabilize or even decrease as VPD rises (Yi *et al* 2019). The primary goal of our study is to characterize these responses over broad gradients in climate and ecosystem types, and to project the magnitude of VPD-driven effects on iWUE into the future.

Meeting this objective has many practical applications. It could help to explain why temporal trends in iWUE inferred at the ecosystem scale from flux towers are higher than expected when considering CO_2 effects alone (Keenan *et al* 2013, Mastrotheodoros *et al* 2017). VPD-effects on iWUE could also partially explain the increasing decoupling of growth and iWUE as observed from tree rings (Andrer-Hayles *et al* 2011, Peñuelas *et al* 2011). A VPD-driven increase in iWUE should not increase tree growth, as overall it will likely be accompanied by lower GPP (Peters *et al* 2018). Finally, our results are relevant for drought monitoring and prediction indices that incorporate information about the difference between potential and actual evapotranspiration (Narasimhan and Srinivasan 2005, Otkin *et al* 2013), which is largely driven by stomatal conductance during dry periods (Novick *et al* 2016a). Therefore, our analysis can clarify how drought-driven declines in conductance translate to declines in GPP, which may ultimately form an important indicator of agricultural drought.

Here, we assessed the extent to which iWUE responds to increasing VPD versus declining soil moisture by leveraging long-term eddy covariance observations of ecosystem-scale C and water exchange from 28 sites representing a broad range of biomes and climate regimes. These data are collected at a timescale (i.e. half-hourly or hourly) over which VPD and soil moisture are typically decoupled (Novick *et al* 2016a), allowing the influence of each on iWUE to be independently assessed. We then projected changes in iWUE to the end of this century by using a VPD dataset downscaled from 15 General Circulation Models (under Representative Concentration Pathway 8.5 (RCP 8.5)—the highest greenhouse gas emission scenario). We also present a theoretical and mathematical framework that facilitates the mechanistic interpretation of results, which is critical for future efforts to represent these dynamics in ecosystem models.

Materials and methods

Tower-derived estimates of ecosystem intrinsic water use efficiency

Intrinsic water use efficiency at the leaf level (iWUE, μmol mol^{-1}) is defined as the ratio of carbon assimilation (A_n, μmol m^{-2} s^{-1}) to stomatal conductance (g_s, mol m^{-2} s^{-1}):

$$\text{iWUE} = \frac{A_n}{g_s}. \quad (1)$$

In this study, the ecosystem-scale intrinsic water use efficiency is estimated at the canopy scale as:

$$\text{iWUE} = \frac{\text{GPP}}{G_s}, \quad (2)$$

noting that iWUE is estimated at the half-hourly or hourly resolution. The high frequency (half-hourly or hourly) data used in this study were obtained from 28 FLUXNET2015 Tier1 dataset sites located in North America (http://fluxnet.fluxdata.org/data/fluxnet2015-dataset/) (see table S1 in the supplementary information-SI is available online at stacks.iop.org/ERL/14/074023/mmedia), which span eight vegetation types and a range of dryness index

(DI = potential evapotranspiration/precipitation; see DI calculation later in this section), noting that each site has at least three years of records. The GPP is gross primary productivity estimated from tower-derived net carbon flux using two partitioning approaches—the so-called 'nighttime approach' (Reichstein *et al* 2005) and 'daytime approach' (Lasslop *et al* 2010); the half-hourly or hourly GPP products were provided by FLUXNET. G_s (m s^{-1}) is surface conductance, which is determined by inverting the Penman–Monteith equation (Monteith 1965) into:

$$G_s = \frac{\gamma \mathrm{LE} g_a}{\Delta(R_n - G) + \rho C_p \mathrm{VPD} g_a - \mathrm{LE}(\Delta + \gamma)}, \quad (3)$$

where Δ(Pa K^{-1}) is the slope of saturated vapor pressure against temperature, R_n−G (W m^{-2}) is available energy—the difference between net radiation (R_n) and ground heat flux (G), ρ (kg m^{-3}) is air density, C_p (J kg^{-1} K^{-1}) is specific heat of air, γ (Pa K^{-1}) is the psychrometric constant, VPD (Pa) is vapor pressure deficit, LE (W m^{-2}) is latent heat flux, and g_a (m s^{-1}) is aerodynamic conductance, quantified by using the Monteith–Unsworth model (Monteith and Unsworth 1990) as

$$g_a = \left(\frac{u}{u^{*2}} + 6.2u^{*-\frac{2}{3}}\right)^{-1}, \quad (4)$$

where u (m s^{-1}) is wind speed at a reference height, and u^* is the friction velocity (m s^{-1}). The unit of surface conductance G_s is converted from [m s^{-1}] into [mol m^{-2} s^{-1}] by multiplying $\frac{P_a}{R \times T_a}$, where P_a (Pa) is air pressure, T_a (K) is air temperature, and R (=8.314 J mol^{-1} K^{-1}) is the gas constant. The FLUXNET2015 dataset includes information on the uncertainty of every half-hourly or hourly water vapor flux measurements (given as a mean and standard deviation), which we propagated through to our derivation of G_s. Specifically, for every half-hourly or hourly estimate of LE, we generated 10 000 estimates drawn from a normal distribution with the mean and standard deviation proposed by FLUXNET. Thus, we also derived 10 000 estimates of G_s, using the mean of this distribution in our analysis.

The Penman–Monteith equation, which describes ecosystem evapotranspiration, relies on a big-leaf assumption, and in many applications G_s is assumed to be equal to the canopy-level surface conductance. However, ecosystem evapotranspiration includes a significant contribution from soil evaporation (typically on the order of 15%–30% for a range of biomes (Wilson *et al* 2001, Oishi *et al* 2010, Wang *et al* 2013, Sulman *et al* 2016)). In modeling studies, this problem is often met with a two-source (i.e. canopy and soil) modeling approach where both canopy and soil evaporation are independently simulated from Penman–Monteith type equations (Shuttleworth and Wallace 1985). However, in data driven applications like this one, when surface conductance is derived by inverting the Penman–Monteith equation from measured ecosystem scale LE observations, the derived G_s is influenced by evaporation from soil and precipitation interception, and should not be assumed to be representative of canopy stomatal conductance alone (Schulze *et al* 1994, Kelliher *et al* 1995, Baldocchi and Meyers 1998, Knauer *et al* 2017a).

To minimize the contribution of surface evaporation to iWUE, and to control for confounding effects from variable leaf area, radiation, and windspeed, the data were subjected to the following set of filters: (1) we only used original measurements (quality control flag = 0) or gap filled data of good quality (quality control flag = 1) as determined by the FLUXNET2015 protocols; (2) the analysis was conducted for periods of relatively stationary Normalized Difference Vegetation Index (NDVI) (https://modis.ornl.gov/fixedsite/) with NDVI > 80%NDVI$_{max}$ (the peak of the annual NDVI series). The NDVI product has a spatial resolution of 250 m, and we used the pixel where the tower resides; (3) the analysis was constrained to 10:00–15:00 local time and only when incoming short-wave radiation (R_s) is higher than 50% of the peak of its annual series (R_{smax}), i.e. $R_s > 50\%R_{smax}$. Note that a discussion of uncertainty introduced by the selection of these two thresholds is provided later in this document; (4) data were filtered to exclude records within two days following rain events (>1 mm) to minimize the contamination of rain on LE measurements; (5) the wind speed was constrained to exceed 1 m s^{-1} to select for periods with negligible leaf boundary layer resistance.

Linking the dynamics of intrinsic water use efficiency to vapor pressure deficit and soil moisture

To disentangle the response of iWUE to changes in soil moisture and VPD, the iWUE determined from equation (2) was averaged within discrete soil moisture and VPD bins. Though soil moisture can sometimes be made at different depths among FLUXNET sites, these measurements are commonly used to characterize the water status of the surface (~the upper 30 cm) soil at FLUXNET sites in cross-site syntheses. Following the approach of Novick *et al* (2016a), the soil moisture bins were set as 15, 30, 50, 70, 90, 100% percentiles of all records, and VPD was binned every 0.2 kPa. We determined a reference GPP (GPP$_{ref}$) and reference conductance (G_{sref}) under conditions of VPD ~1 kPa and soil moisture >90% of the site-specific saturation value. We then normalized the tower-derived GPP and G_s by the reference values to facilitate a cross-site comparison of the relationship of each to VPD. To evaluate the uncertainty associated with the R_s and NDVI filters (NDVI > 80%NDVI$_{max}$ and $R_s > 50\%R_{smax}$), we ran the following two tests: (1) we modified the NDVI filter to NDVI > 60%NDVI$_{max}$ while maintaining $R_s > 50\%R_{smax}$; (2) we modified R_s filter to

$R_s > 70\%R_{smax}$ while maintaining $NDVI > 80\%NDVI_{max}$.

To avoid confounding effects introduced by covariation of VPD and CO_2 concentrations, we repeated the analysis but filtered the data into three bins associated with unique ranges of CO_2 concentration (365 to 375 ppm, 370 to 380 ppm, and 375 to 385 ppm). This approach allows us to evaluate if the response of iWUE to VPD is robust to changes in CO_2 concentration.

Using dryness index to facilitate cross-site trend analysis

We linked cross-site trends in the dynamics of iWUE to the Dryness Index (DI), defined as the ratio of mean annual potential evapotranspiration (PET) to mean annual precipitation (P):

$$DI = \frac{PET}{P}. \quad (5)$$

We used the Priestley–Taylor equation (Priestley and Taylor 1972) to determine PET, which is well-correlated with PET derived from the more mechanistically complete but data-demanding Penman–Monteith equation (Novick *et al* 2016a). The Priestley–Taylor equation takes the form:

$$PET = \alpha_{PT}\frac{\Delta R_n}{\lambda(\Delta + \gamma)}, \quad (6)$$

where $\alpha_{PT} = 1.26$ is the Priestley–Taylor coefficient, and λ is the latent heat of vaporization.

The DI is usually used to quantify the 'dryness' of a landscape. At sites where DI is lower than 1, annual precipitation is higher than potential evapotranspiration, indicating excess water for soil moisture recharge and runoff generation. In such conditions, plants are not limited by water availability (except in seasonally dry climates). When DI is higher than 1, most of the annual precipitation is turned into evapotranspiration, leaving plants limited by water availability. We calculated the DI using the long-term mean annual precipitation (see table S1) reported by each site to the FLUXNET Database (http://fluxnet.ornl.gov/) instead of calculating mean annual precipitation from the FLUXNET2015 high frequency dataset, which is sensitive to missing records. Note that for US-AR1 and US-AR2 sites, where no annual precipitation was provided in the FLUXNET Database, we used the high frequency precipitation records in the FLUXNET2015 dataset.

Historic and projected VPD

Bias-corrected and downscaled (~4 km grid) General Circulation Model (GCM) projections for each site in the US were extracted from the Multivariate Adaptive Constructed Analogs—version 2 (MACA (Abatzoglou and Brown 2012)) data warehouse (http://maca.northwestknowledge.net/). Specifically, daily maximum and minimum air temperature and maximum and minimum relative humidity from 15 GCMs (table S2) were extracted from the Coupled Model Intercomparison Project—Phase 5 (CMIP5 (Taylor *et al* 2012)) archive for Representative Concentration Pathway 8.5 (the highest greenhouse gas emission scenario) from 1950–2099. First, the daily maximum and minimum saturated vapor pressures were calculated using the maximum and minimum air temperatures, respectively, and then averaged to calculate the daily saturated vapor pressure. Second, the actual vapor pressure was calculated by multiplying the daily saturated vapor pressure and the daily relative humidity estimated from daily maximum and minimum relative humidity (Allen *et al* 1998). Finally, daily averaged VPD was calculated by subtracting the daily actual vapor pressure from the daily saturated vapor pressure. To account for the uncertainty of air temperature and relative humidity in the projections, VPD of the 15 different GCMs were averaged for each site in this analysis. The VPD generally exhibits an increasing trend in all sites (figure S1) as a result of the rising temperature (figure S2) and relatively steady or slightly declining relative humidity (figure S3).

Quantifying the sensitivity of iWUE and GPP to VPD

When VPD is relatively low and conductance is relatively high, a positive relationship between iWUE and VPD is expected, as conductance declines swiftly with rising VPD, but assimilation is relatively insensitive to the changes in conductance, since intercellular CO_2 concentrations remain high. However, as VPD continues to increase and conductance continues to decrease, reductions in intercellular CO_2 will begin to limit photosynthesis, either alone or together with other non-stomatal limitations if soil moisture also decreases (Lawlor and Tezara 2009, Novick *et al* 2016b). Thus, the relationship between iWUE and VPD may be linear, hyperbolic, or even unimodal depending on how hydrologic stress limits the transfer of CO_2 from the air to the chloroplast. Therefore, we fit the iWUE-VPD relationship to a second order polynomial curve because it can accommodate the entire range of responses that may be expected across the wide range of sites considered here:

$$iWUE = aVPD^2 + bVPD + c, \quad (7)$$

where a, b and c are parameters that were optimized by using the least square method and listed in table S3. It follows that the sensitivity of iWUE to VPD ($=\partial iWUE/\partial VPD$) may be expressed as $2aVPD+b$.

The change in iWUE as VPD rises can mitigate, or buffer, drought-driven reductions in GPP caused by reduced conductance or decreased photosynthetic capacity. To quantify this effect across sites, we expressed GPP as the product of iWUE and G_s while neglecting the CO_2 effects

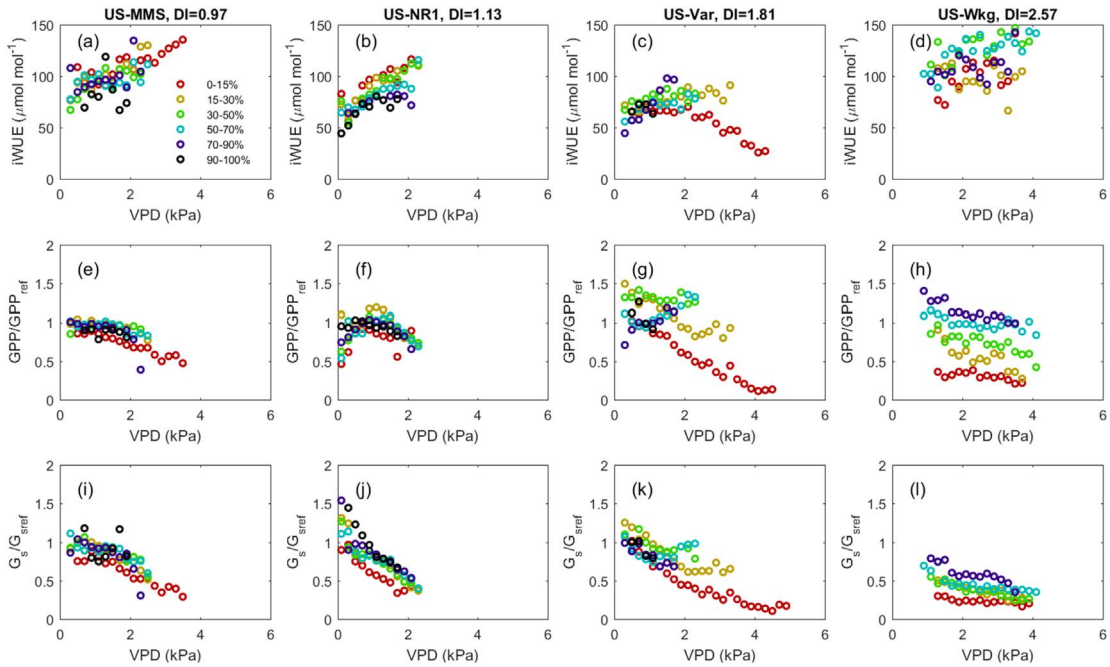

Figure 1. In most sites, and for most soil moisture classes, intrinsic water use efficiency (iWUE) initially rises with increasing vapor pressure deficit (VPD) (a)–(d), reflecting declines in surface conductance (G_s) (i)–(l) that are not accompanied by similar limitations to GPP (e)–(h). Representative sites are selected to show results with contrasting dryness index (quantified as the ratio of potential evapotranspiration and precipitation; see Materials and Methods) from mesic (DI = 0.97 in US-MMS) to arid (DI = 2.57 in US-Wkg) sites. Both G_s and GPP were normalized by reference values (G_{sref} and GPP_{ref}, respectively) recorded at VPD = 1 kPa under well-watered conditions. Data of different colors are shown for soil moisture bins in percentiles (see Materials and Methods). The US-MMS site is Deciduous Broadleaf Forest, the US-NR1 site is Evergreen Needleleaf Forest, and US-Var and US-Wkg sites are Grasslands. Note that each dot here represents the average of all the half-hourly or hourly data samples in each soil moisture and VPD bin.

$$\mathrm{GPP} = \mathrm{iWUE} \times G_s. \tag{8}$$

The full derivative of GPP with respect to VPD is thus:

$$\frac{\mathrm{dGPP}}{\mathrm{dVPD}} = \frac{\partial G_s}{\partial \mathrm{VPD}}\mathrm{iWUE} + \frac{\partial \mathrm{iWUE}}{\partial \mathrm{VPD}}G_s, \tag{9}$$

where $\frac{\partial G_s}{\partial \mathrm{VPD}}\mathrm{iWUE}$ is the sensitivity of GPP to VPD linked to stomatal closure, whereas $\frac{\partial \mathrm{iWUE}}{\partial \mathrm{VPD}}G_s$ is the sensitivity of GPP to VPD linked to rising iWUE.

Here, the relationship between G_s and VPD was assumed to have the form proposed by Oren *et al* (1999):

$$G_s = G_{s\mathrm{REF}} - m \ln(\mathrm{VPD}), \tag{10}$$

where $G_{s\mathrm{REF}}$ is the reference conductance when VPD = 1 kPa, and m describes the sensitivity of conductance to VPD; both parameters were optimized by using the least square method and listed in table S4. The F-test was used to evaluate the significance of regressions.

Results and discussion

Response of intrinsic water use efficiency to hydrologic stress

As hydrologic stress developed at each site, we observed a nearly universal initial increase in iWUE that was primarily driven by rising VPD (see figures 1(a)–(d) for representative sites with contrasting DI; figures S4 and S5 in the SI for all sites). Within each site, the initial increase of iWUE to VPD was observed across all soil moisture conditions, indicating a robust positive control of VPD on iWUE. Additionally, no detectable trend was found in the relationship between iWUE and soil moisture under the same VPD levels (figure S6), underscoring the critical role of VPD in regulating iWUE during drought. Notably, the increases in iWUE were driven by decreases in G_s (figures 1(i)–(l); S7 for all sites), rather than by changes in GPP (figures 1(e)–(h); S8 for all sites). Because the partitioning method did not strongly affect results when comparing figures S4 with S5 in SI, here and throughout, we focus on trends in GPP estimated using the so-called 'nighttime approach' by Reichstein *et al* (2005). The uncertainty associated with the R_s and NDVI filters ($\mathrm{NDVI} > 80\%\mathrm{NDVI}_{\max}$ and $R_s > 50\%R_{s\max}$) is negligible, because when we changed the threshold of NDVI and R_s filters, similar results were achieved (see figures S9 and S10). Therefore, the filter choice does not appear to strongly influence results and we only focus the analysis under the filter scheme of $\mathrm{NDVI} > 80\%\mathrm{NDVI}_{\max}$ and $R_s > 50\%R_{s\max}$.

In many biomes, the increase in iWUE with rising VPD did not continue unabated, and a near-hyperbolic relationship emerged; in a few cases, a unimodal relationship between iWUE and VPD was observed

(e.g. US-Var site in figure 1) characterized by a clear maximum iWUE under intermediate VPD. To describe the full range of the iWUE response to VPD at each site, we parameterized a second order polynomial model for the relationship between iWUE and VPD regardless of soil moisture conditions (see method section and table S3 for details). In addition, to better understand the initial iWUE increase with rising VPD, we estimated the slope of the iWUE-VPD relationship at a relatively low reference VPD (VPD = 1 kPa). Our results confirm that an initial positive relationship between iWUE and VPD is common across sites (figure S11(a)). Next, by analyzing the slope of the iWUE-VPD relationship when VPD was at its site-specific maxima across all sites, we further showed that most sites continue to exhibit an increasing iWUE trend in response to VPD even when VPD is high (figure S11(b)). To understand the influence of vegetation type versus climate on iWUE-VPD relationship, we averaged both slopes by the IGBP vegetation type (see figure S12), and found the initial slope of iWUE to VPD in Closed Shrublands is the lowest, while that of Mixed Forest is the highest (figure S12(a)). Though an initial increase of iWUE is found across all vegetation types, when VPD is at the site maxima, the slope becomes substantially lower in most vegetation types and even negative in grasslands (figure S12(b)), however, in Closed Shrublands and Deciduous Broadleaf Forests the slope increases. While the initial slope of the iWUE-VPD relationship exhibits no clear dependence on DI (figure S13(a)), the slope calculated at the site VPD maxima showed a weak negative correlation with DI (figure S13(b)). In other words, the iWUE tends to decrease under high VPD conditions at arid sites.

The initial iWUE increase in response to rising VPD reflects the relatively slower decrease in GPP compared to the rapid decrease in G_s as VPD rises. To reiterate, these different patterns between GPP and G_s can be understood by considering the leaf-level processes that control gas exchange. When internal CO_2 concentration is high (as is the case when G_s is high), photosynthesis is less sensitive to small changes in internal CO_2 concentration and will therefore show relatively little response to a decrease in stomatal conductance, leading to the increasing iWUE at low to moderate VPD shown in figure 1. As stomata close while VPD further increases (Oren *et al* 1999), leaf internal CO_2 concentration continues to decline; at these lower intercellular CO_2 concentrations, photosynthesis declines rapidly with decreasing CO_2 availability, and iWUE no longer rises with increasing VPD (Farquhar and Sharkey 1982). However, if conditions associated with high VPD suppress photosynthetic capacity, such as high temperatures (Yamori *et al* 2014) or low leaf water potentials (Lawlor and Tezara 2009) that develop in dry conditions, photosynthetic capacity can be inhibited, lowering the demand for CO_2 and stabilizing the atmosphere-leaf CO_2 concentration gradient to lower values. When inhibition of photosynthesis develops, iWUE begins to decrease, as seen at high VPD and low soil moisture conditions (e.g. US-Var in figure 1; also US-SRM and US-AR1 in figure S4).

Assessing the sensitivity of GPP to VPD

The contrasting response of iWUE and G_s to VPD raises the question: to what extent does high VPD ultimately limit GPP? The sensitivity analysis described in equations (8)–(10) allows us to quantify when and where VPD-driven reductions in conductance translate into reductions in GPP. We found that stomatal conductance declines monotonically with increasing VPD (figures 1(i)–(l); S7 for all sites); thus, the $\frac{\partial G_s}{\partial \mathrm{VPD}}\mathrm{iWUE}$ component of equation (9) is always negative (blue line in figure 2), thereby driving a decrease in GPP. However, $\frac{\partial \mathrm{iWUE}}{\partial \mathrm{VPD}}G_s$ is typically positive under low VPD levels (magenta line in figure 2). Or in other words, GPP is less sensitive to VPD than is conductance (figure 1). Overall, GPP exhibits a net decline in response to increasing VPD (green line in figure 2), but of a magnitude that is less severe than that predicted from stomatal closure alone regardless of local climate (figures 2(b)–(f) with contrasting DI).

Projecting intrinsic water use efficiency into the future

VPD is already rising in many places (Ficklin and Novick 2017), driven by increases in the saturated vapor pressure that are not matched by concurrent increases in actual vapor pressure. To quantify the potential for varying VPD to drive both historic and future changes in iWUE, we used site-specific relationships between iWUE and VPD (figure S4 and table S3) and estimated an upper limit on the extent to which rising VPD due to climate change could affect future relationships between photosynthesis and stomatal conductance. Using daily VPD records and projected VPD trends from a downscaled and bias-corrected General Circulation Model ensemble (15 models; table S2) together with the aforementioned iWUE-VPD relationship, we estimated historic changes in iWUE and projected iWUE values into the future for each site (figure 3; see figure S14 for the variation resulting from the 15 GCM products at each site). Because these projections are based on iWUE-VPD relations, they do not include any CO_2 effect.

Most sites showed an increasing trend in iWUE relative to the average of 1950–1960. In particular, our results suggest that rising VPD will increase iWUE by 5%–15% (relative to the 1950–1960 baseline) in many sites by 2050, and by 10%–35% in the majority of sites by the end of the century (figure 3). These increases in iWUE are not as large as those expected from future elevated CO_2, which are on the order of 50%–70% for CO_2 concentrations of 540–570 ppm suggested by tree

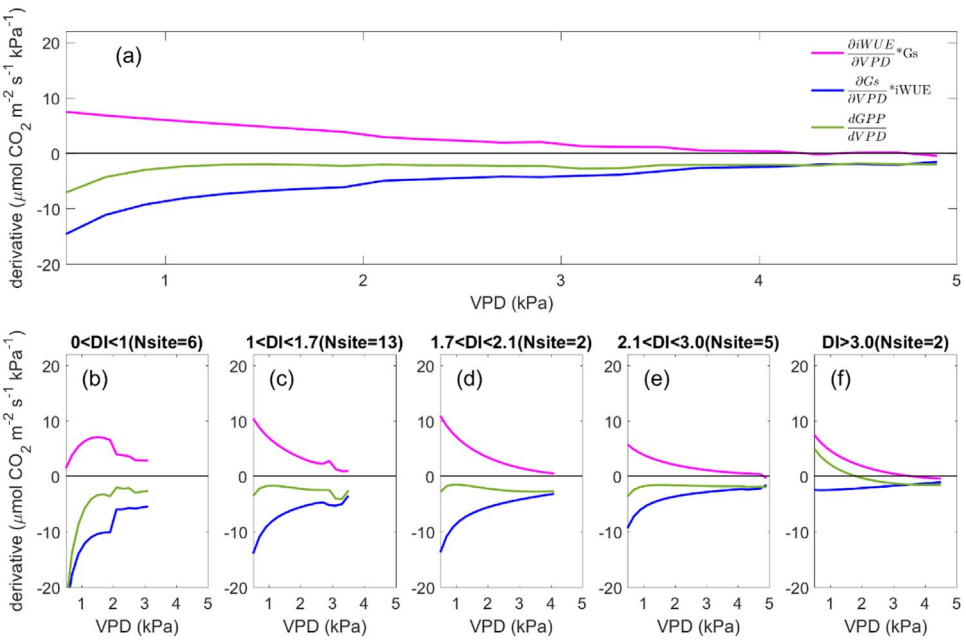

Figure 2. The sensitivity of gross primary productivity (GPP) to vapor pressure deficit (VPD) caused by reduced conductance tends to lower GPP during drought ($\frac{\partial G_s}{\partial \mathrm{VPD}}$iWUE; blue line), whereas the sensitivity of GPP to VPD linked to rising intrinsic water use efficiency (iWUE) tends to increase GPP during drought ($\frac{\partial \mathrm{iWUE}}{\partial \mathrm{VPD}}G_s$; magenta lines). The net sensitivity of GPP to VPD ($\frac{d\mathrm{GPP}}{d\mathrm{VPD}}$) is negative (shown in green). Upper panel (a) is the average of all 28 sites, and bottom panels (b)–(f) are the averages under different dryness index (DI) levels.

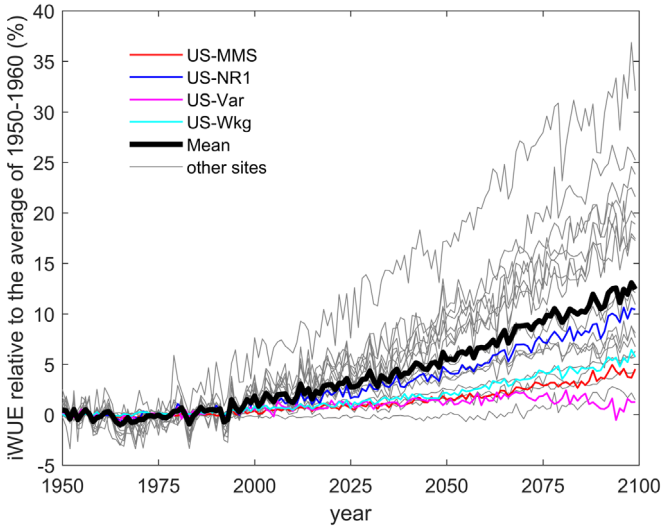

Figure 3. Reconstructed historic and projected future increases in intrinsic water use efficiency (iWUE) (relative to the average of 1950–1960) as driven by vapor pressure deficit (VPD). These projections were derived by forcing the site-specific polynomial models with an averaged General Circulation Model ensemble projections for VPD at the site level. Each gray line represents an individual site with the representative sites of figure 1 highlighted by colors, and the thick black line represents an average of all sites.

ring core analysis in Free-Air CO_2 enrichment (FACE) experimental conditions (Battipaglia *et al* 2013). However, at least in some sites, the magnitude of projected increases in iWUE due to VPD alone is still substantial. Our results also indicate a 0.13% year^{-1} increasing rate is expected for iWUE in the future owing to the rising VPD associated with the elevated global temperatures.

Excluding the CO_2 contamination effect

To ensure that our results (figures 1 and S4) are not biased by co-occurring changes in CO_2, we repeated the analysis using data constrained to a narrow range of CO_2. After reducing the effects of CO_2, our results exhibited the same hyperbolic iWUE-VPD relationship (figures S15–17). These results are consistent with previous results (Keenan *et al* 2013, Mastrotheodoros *et al* 2017) reporting that tower-derived iWUE trends

are higher than expected when considering CO_2 effects alone. Specifically, Mastrotheodoros *et al* (2017) used a model to show that consideration of changes in humidity and temperature better reconcile apparent iWUE trends with those predicted from CO_2 effects alone. Our study now offers an empirical analysis in support of those model predictions. This result implies that attributing the historic increase in iWUE to rising CO_2 alone is challenging, at least at the fine timescale (~hourly) of the data used in this study, and that VPD in addition to rising CO_2 is likely to be a significant driver of historic and future increases in iWUE. Finally, our results show that increased iWUE driven by higher VPD usually corresponds with a reduced GPP (figures 1(e)–(h)), different from increased iWUE under elevated CO_2 that results from increased GPP. Thus, an increase in iWUE does not necessarily translate into increased carbon uptake as simulated by land surface models (Peters *et al* 2018) or increased tree growth as reported by tree ring data (Lévesque *et al* 2014, van der Sleen *et al* 2015), or in other words, whether higher iWUE corresponds to higher GPP depends on the driver of iWUE changes.

Conclusion

Intrinsic water use efficiency has long been recognized as a key parameter linking the global C and water cycles. However, the effect of atmospheric demand on ecosystem iWUE has rarely been quantified when analyzing historic iWUE data or predicting iWUE trends into the future. We show that, when VPD is relatively low, iWUE increases with rising VPD across a wide range of biomes. Whether this increase persists under high VPD depends on climate regime, among other factors. Our work suggests that the historic sensitivity of iWUE to rising CO_2 (Feng 1999, Keenan *et al* 2013) may be overestimated in places where VPD has also been rising and may explain previously contradictory results of spatial heterogeneity in iWUE patterns (Marshall and Monserud 1996, Keenan *et al* 2013, Wu *et al* 2015). The increase in iWUE may not necessarily translate into increase in tree growth, as a VPD-driven increase in iWUE is not accompanied by an increase in GPP. In fact, GPP tends to decline with rising VPD, but as our results show, the magnitude of this decline is less substantial when compared to VPD-driven declines in conductance.

Acknowledgments

The authors thank J S Dukes, S Kannenberg, M Craig, A Keller, R Mushinski, and K Beidler for constructive feedback on earlier versions of the manuscript, and M L Virdi for the help with MODIS NDVI data. We thank two anonymous reviewers for their constructive comments that lead to substantial improvement of this paper. We acknowledge the World Climate Research Programme's Working Group on Coupled Modelling, which is responsible for the Coupled Model Intercomparison Project (CMIP). We acknowledge the US Department of Energy for its support of the Ameriflux Management Project and FLUXNET, and thank AmeriFlux PIs for sharing their data. This work was supported by the NSF DEB grant 1552747, NASA–ROSES grant NNX17AE69G, and USDA AFRI award-2017-67013-26191. SM acknowledges partial support from the Swedish Research Council Formas (2016-00998 and 2018-00968), and DW acknowledges support from an NSERC Discovery Grant.

Author contributions

QZ and KAN designed the study and methodology, with substantial input from all co-authors, especially DLF, who processed the future climate projections of vapor pressure deficit. All authors contributed to interpretation of results. QZ and KAN drafted the manuscript. All authors edited and approved the final manuscript.

Competing financial interests

The authors declare no competing financial interests.

ORCID iDs

Quan Zhang https://orcid.org/0000-0003-1127-5969

References

Abatzoglou J T and Brown T J 2012 A comparison of statistical downscaling methods suited for wildfire applications *Int. J. Climatol.* **32** 772–80

Ainsworth E A and Long S P 2005 What have we learned from 15 years of free-air CO_2 enrichment (FACE)? A meta-analytic review of the responses of photosynthesis, canopy *New Phytol.* **165** 351–71

Allen R G, Pereira L S, Raes D and Smith M 1998 Crop eva potranspiration-Guidelines for computing crop water requirements-FAO Irrigation and drainage paper 56 FAO, Rome 300 D05109

Andrer-Hayles L *et al* 2011 Long tree-ring chronologies reveal 20th century increases in water-use efficiency but no enhancement of tree growth at five Iberian pine forests *Glob. Change Biol.* **17** 2095–112

Baldocchi D and Meyers T 1998 On using eco-physiological, micrometeorological and biogeochemical theory to evaluate carbon dioxide, water vapor and trace gas fluxes over vegetation: a perspective *Agric. Forest Meteorol.* **90** 1–25

Battipaglia G *et al* 2013 Elevated CO_2 increases tree—level intrinsic water use efficiency: insights from carbon and oxygen isotope analyses in tree rings across three forest FACE sites *New Phytol.* **197** 544–54

Farquhar G and Wong S 1984 An empirical model of stomatal conductance *Funct. Plant Biol.* **11** 191–210

Farquhar G D, Oleary M H and Berry J A 1982 On the relationship between carbon isotope discrimination and the inter-cellular carbon-dioxide concentration in leaves *Aust. J. Plant Physiol.* **9** 121–37

Farquhar G D and Sharkey T D 1982 Stomatal conductance and photosynthesis *Annu. Rev. Plant Physiol.* **33** 317–45
Feng X H 1999 Trends in intrinsic water-use efficiency of natural trees for the past 100–200 years: a response to atmospheric CO_2 concentration *Geochim. Cosmochim. Acta* **63** 1891–903
Ficklin D L and Novick K A 2017 Historic and projected changes in vapor pressure deficit suggest a continental-scale drying of the United States atmosphere *J. Geophys. Res.-Atmos.* **122** 2061–79
Frank D C *et al* 2015 Water-use efficiency and transpiration across European forests during the anthropocene *Nat. Clim. Change* **5** 579–83
Franks P J *et al* 2013 Sensitivity of plants to changing atmospheric CO_2 concentration: from the geological past to the next century *New Phytol.* **197** 1077–94
Gomes F P *et al* 2009 Is abscisic acid involved in the drought responses of Brazilian green dwarf coconut? *Exp. Agric.* **45** 189–98
Keenan T F *et al* 2013 Increase in forest water-use efficiency as atmospheric carbon dioxide concentrations rise *Nature* **499** 324–8
Kelliher F M, Leuning R, Raupach M R and Schulze E D 1995 Maximum conductances for evaporation from global vegetation types *Agric. Forest Meteorol.* **73** 1–16
Knauer J *et al* 2017a Towards physiologically meaningful water-use efficiency estimates from eddy covariance data *Global Change Biol.* **24** 694–710
Knauer J *et al* 2017b The response of ecosystem water-use efficiency to rising atmospheric CO_2 concentrations: sensitivity and large-scale biogeochemical implications *New Phytol.* **213** 1654–66
Kwon H, Law B E, Thomas C K and Johnson B G 2017 The influence of hydrological variability on inherent water use efficiency in forests of contrasting composition, age, and precipitation regimes in the Pacific Northwest *Agric. Forest Meteorol.* **249** 488–500
Lasslop G *et al* 2010 Separation of net ecosystem exchange into assimilation and respiration using a light response curve approach: critical issues and global evaluation *Glob. Change Biol.* **16** 187–208
Lawlor D W and Tezara W 2009 Causes of decreased photosynthetic rate and metabolic capacity in water-deficient leaf cells: a critical evaluation of mechanisms and integration of processes *Ann. Bot.* **103** 561–79
Lévesque M, Siegwolf R, Saurer M, Eilmann B and Rigling A 2014 Increased water-use efficiency does not lead to enhanced tree growth under xeric and mesic conditions *New Phytol.* **203** 94–109
Marshall J D and Monserud R A 1996 Homeostatic gas-exchange parameters inferred from $^{13}C/^{12}C$ in tree rings of conifers *Oecologia* **105** 13–21
Mastrotheodoros T *et al* 2017 Linking plant functional trait plasticity and the large increase in forest water use efficiency *J. Geophys. Res.-Biogeosci.* **122** 2393–408
Monteith J L 1965 Evaporation and environment *Symp. Soc. Exp. Biol.* pp 205–34
Monteith J L and Unsworth M H 1990 *Principles of Environmental Physics* ed E Arnold (London: Routledge)
Narasimhan B and Srinivasan R 2005 Development and evaluation of soil moisture deficit index (SMDI) and evapotranspiration deficit index (ETDI) for agricultural drought monitoring *Agric. Forest Meteorol.* **133** 69–88
Novick K A *et al* 2016a The increasing importance of atmospheric demand for ecosystem water and carbon fluxes *Nat. Clim. Change* **6** 1023–7
Novick K A, Miniat C F and Vose J M 2016b Drought limitations to leaf-level gas exchange: results from a model linking stomatal optimization and cohesion-tension theory *Plant Cell Environ.* **39** 583–96
Oishi A C, Oren R, Novick K A, Palmroth S and Katul G G 2010 Interannual invariability of forest evapotranspiration and its consequence to water flow downstream *Ecosystems* **13** 421–36
Oren R *et al* 1999 Survey and synthesis of intra-and interspecific variation in stomatal sensitivity to vapour pressure deficit *Plant Cell Environ.* **22** 1515–26
Otkin J A *et al* 2013 Examining rapid onset drought development using the thermal infrared–based evaporative stress index *J. Hydrometeorol.* **14** 1057–74
Peters W *et al* 2018 Increased water-use efficiency and reduced CO_2 uptake by plants during droughts at a continental scale *Nat. Geosci.* **11** 744–8
Peñuelas J, Canadell J G and Ogaya R 2011 Increased water-use efficiency during the 20th century did not translate into enhanced tree growth *Glob. Ecol. Biogeogr.* **20** 597–608
Priestley C and Taylor R 1972 On the assessment of surface heat flux and evaporation using large-scale parameters *Mon. Weather Rev.* **100** 81–92
Reichstein M *et al* 2005 On the separation of net ecosystem exchange into assimilation and ecosystem respiration: review and improved algorithm *Glob. Change Biol.* **11** 1424–39
de Santana T A *et al* 2015 Water use efficiency and consumption in different Brazilian genotypes of Jatropha curcas L. subjected to soil water deficit *Biomass Bioenergy* **75** 119–25
Schultz H R and Stoll M 2010 Some critical issues in environmental physiology of grapevines: future challenges and current limitations *Aust. J. Grape Wine Res.* **16** 4–24
Schulze E D, Kelliher F M, Korner C, Lloyd J and Leuning R 1994 Relationships among maximum stomatal conductance, ecosystem surface conductance, carbon assimilation rate, and plant nitrogen nutrition—a global ecology scaling exercise *Annu. Rev. Ecol. Syst.* **25** 629–60
Shuttleworth W J and Wallace J 1985 Evaporation from sparse crops —an energy combination theory *Q. J. R. Meteorol. Soc.* **111** 839–55
van der Sleen P *et al* 2015 No growth stimulation of tropical trees by 150 years of CO_2 fertilization but water-use efficiency increased *Nat. Geosci.* **8** 24–8
Sulman B N, Roman D T, Scanlon T M, Wang L X and Novick K A 2016 Comparing methods for partitioning a decade of carbon dioxide and water vapor fluxes in a temperate forest *Agric. Forest Meteorol.* **226** 229–45
Taylor K E, Stouffer R J and Meehl G A 2012 An overview of CMIP5 and the experiment design *Bull. Am. Meteorol. Soc.* **93** 485–98
Tomas M *et al* 2014 Variability of water use efficiency in grapevines *Environ. Exp. Bot.* **103** 148–57
Wang L X *et al* 2013 The effect of warming on grassland evapotranspiration partitioning using laser-based isotope monitoring techniques *Geochim. Cosmochim. Acta* **111** 28–38
Wieser G *et al* 2016 Stable water use efficiency under climate change of three sympatric conifer species at the alpine treeline *Frontiers Plant Sci.* **7**
Wilson K B, Hanson P J, Mulholland P J, Baldocchi D D and Wullschleger S D 2001 A comparison of methods for determining forest evapotranspiration and its components: sap-flow, soil water budget, eddy covariance and catchment water balance *Agric. Forest Meteorol.* **106** 153–68
Wu G J *et al* 2015 Elevation-dependent variations of tree growth and intrinsic water-use efficiency in Schrenk spruce (Picea schrenkiana) in the western Tianshan Mountains, China *Frontiers Plant Sci.* **6**
Yamori W, Hikosaka K and Way D A 2014 Temperature response of photosynthesis in C3, C4, and CAM plants: temperature acclimation and temperature adaptation *Photosynth. Res.* **119** 101–17
Yi K *et al* 2019 Linking variation in intrinsic water-use efficiency to isohydricity: a comparison at multiple spatiotemporal scales *New Phytol.* **221** 195–208